Available online at www.sciencedirect.com

SCIENCE DIRECT

Developmental Biology 272 (2004) 470–482

DEVELOPMENTAL BIOLOGY

www.elsevier.com/locate/ydbio

Cell autonomy of the mouse *claw paw* mutation

Aysel Darbas,[a,1] Martine Jaegle,[a,1] Erik Walbeehm,[b] Hans van den Burg,[c] Siska Driegen,[a,c] Ludo Broos,[a] Matthijs Uyl,[a] Pim Visser,[a] Frank Grosveld,[a] and Dies Meijer[a,*]

[a] *Department of Cell Biology and Genetics, ErasmusMC, Erasmus University Medical Center, 3000DR Rotterdam, Netherlands*
[b] *Department of Reconstructive Surgery, ErasmusMC, Erasmus University Medical Center, 3000DR Rotterdam, Netherlands*
[c] *Department of Neurosciences, ErasmusMC, Erasmus University Medical Center, 3000DR Rotterdam, Netherlands*

Received for publication 4 March 2004, revised 21 May 2004, accepted 21 May 2004

Abstract

Mice homozygous for the autosomal recessive mutation *claw paw* (*clp*) are characterized by limb posture abnormalities and congenital hypomyelination, with delayed onset of myelination of the peripheral nervous system but not the central nervous system. Although this combination of limb and peripheral nerve abnormalities in *clp/clp* mice might suggest a common neurogenic origin of the syndrome, it is not clear whether the *clp* gene acts primarily in the neurone, the Schwann cell or both. In the work described here, we address this question of cell autonomy of the *clp* mutation through reciprocal nerve grafting experiments between wild-type and *clp/clp* animals. Our results demonstrate that the *clp* mutation affects the Schwann cell compartment and possibly also the neuronal compartment. These data suggest that the *clp* gene product is expressed in Schwann cells as well as neurones and is likely to be involved in direct axon–Schwann cell interactions. Within the Schwann cell, *clp* affects a myelin-related signaling pathway that regulates periaxin and Krox-20 expression, but not Oct-6.

Keywords: Myelination; Schwann cell; Arthrogryposis; POU factors; Periaxin

Introduction

Congenital limb posture abnormalities in humans and other vertebrates occur under a variety of circumstances and clinically manifest as a singular abnormality or as part of a syndrome. In clinical practice, such abnormalities are described as arthrogryposis multiplex congenita (AMC; arthron = "joint" and gryposis = "bent"). It is generally accepted that any condition resulting in reduced fetal movement will lead to joint contractures in newborns (Drachman, 1971; Hageman and Willemse, 1983; Hall, 1997). In principle, such conditions could be extrinsic or intrinsic to the developing fetus. An example of the former is provided by experiments in which chick or rat embryos were paralyzed by injection with curare, causing limb posture abnormalities at birth (Del Torto et al., 1983; Drachman and Coulombre, 1962; Moessinger, 1983). Additionally, maternal antibodies that functionally inhibit the fetal acetylcholine receptor cause arthrogryposis in human fetuses (Jacobson et al., 1999; Matthews et al., 2002; Polizzi et al., 2000).

Intrinsic causes of reduced fetal movement can be classified as either myogenic and/or neurogenic in origin. In several clinical cases, AMC was found associated with congenital hypomyelination of the peripheral nerves suggesting a common aetiology (Boylan et al., 1992; Charnas et al., 1988; Seitz et al., 1986). In the peripheral nervous system, myelin formation and maintenance of the peripheral nervous system by Schwann cells is dependent on continuous reciprocal interactions between the axon and Schwann cell (Fields and Stevens-Graham, 2002). Mutations that affect this dialogue by disabling function in the Schwann cell, the axon or in both result in dys- or demyelinating neuropathies as in the human hereditary motor and sensory neuropathies (Suter and Scherer, 2003). Limb posture abnormalities, mostly pes cavus, and distal muscle wasting frequently develop in these patients as consequence of axonal loss.

Congenital limb posture abnormalities are observed in mice homozygous for the murine autosomal recessive mutation *claw paw* (*clp*) (Henry et al., 1991). In affected

* Corresponding author. Department of Cell Biology and Genetics, ErasmusMC, Erasmus University Medical Center, Dr Molewaterplein 50, PO Box 1738, 3000DR Rotterdam, Netherlands. Fax: +31-10-408-9468.
E-mail address: d.meijer@erasmusmc.nl (D. Meijer).
[1] These authors contributed equally to this study.

0012-1606/$ - see front matter © 2004 Elsevier Inc. All rights reserved.
doi:10.1016/j.ydbio.2004.05.017

animals, the forelimbs are flexed at one or more of the joints (shoulder, wrist or digital joints) but extended at the elbow, resulting in the forelimbs pointing in the direction of the hindlimbs. These abnormalities are visible within 2 days of birth. More severely affected animals also show involvement of one or both hindlimbs. Pathological examination of affected animals demonstrates severe congenital hypomyelination with delayed onset of myelination of the peripheral nerves with central nerves unaffected. Persistently blocked myelination is observed in a fraction of the smaller axons (Henry et al., 1991). Additionally, it was found that the mean internodal length is greatly reduced for all axonal size classes in *clp/clp* nerves when compared to heterozygous or wild-type animals (Koszowski et al., 1998). The *clp* gene has not been identified yet, although mapping studies have placed the gene close to the *Gpi* locus on mouse chromosome 7 (Henry et al., 1991). No mutations were found in the *myelin-associated glycoprotein* (*MAG*) gene, close to the *Gpi* locus, excluding this gene as a *clp* candidate (Niemann et al., 1998). The pathology of the *clp/clp* mouse is strikingly similar to the clinically described cases of AMC mentioned above. Hence, *clp/clp* mice provide an opportunity to study the basis of the relationship between arthrogryposis and hypomyelination.

It has been hypothesized that the *clp* gene is part of the neurone–glia signaling system that governs myelination initiation during development. However, it is not known what cellular and molecular components of this signaling system are affected by the *clp* mutation. To further characterize this mutant mouse, we set out to determine whether the gene acts in the neurone, the Schwann cell or both, through reciprocal nerve graft experiments. Additionally, we studied the interaction of the *clp* gene with many known Schwann cell autonomous regulatory genes involved in myelination including the transcription factors *Oct-6* and *Krox-20* (Topilko and Meijer, 2001). Our results indicate that *clp* function is required within the Schwann cell as well as in the neurone. Upregulation of the promyelin transcription factor Oct-6 is not affected by *clp*, while the subsequent Krox-20 activation is delayed. Additionally, embryonic periaxin expression is absent or reduced in *clp/clp* Schwann cells and postnatal expression is delayed. Taken together, these results suggest that *clp* is involved in neurone–glia interactions and furthermore that, within the Schwann cell, *clp* is involved in a pathway that regulates periaxin and Krox-20 expression. This *clp*-dependent pathway is parallel and non-redundant to the myelin-related Oct-6-dependent pathway.

Materials and methods

Animal surgery

Nerve crush experiments were performed on young adult F2 animals from a C57BL6J/Balbc-*clp* heterozygous intercross. Affected and non-affected mice were anesthetized by inhalation of halothane and placed on a heating pad. The left sciatic nerve was exposed and crushed for two times 15 s at mid-femoral level using No.5 Biology forceps. Mice were sacrificed 4 weeks after the operation through trans-cardiac perfusion with a solution of 1% gluteraldehyde/3% paraformaldehyde in 100 mM cacodylate (pH 7.4). The operated and contralateral nerve was isolated for light and electron microscopic analysis.

Transplantation experiment

Reciprocal nerve grafting experiments were performed between wild type and wild type (wt:wt), wild type and *clp/clp* (wt:clp), *clp/clp* and wild type (clp:wt) and between *clp/clp* and *clp/clp* (clp:clp). All animals were of C57BL6J background, obviating the use of immune-suppressants to prevent graft rejection. Operations were performed on two animals at a time, both animals serving as nerve donor and recipient. Two mice of appropriate genotype were anesthetized through inhalation of halothane and placed on a heating pad. The left sciatic nerve was exposed in both animals. Approximately 7.5 –10 mm of nerve was excised and placed in the same orientation in the host animal. Nerve and muscle tissue were kept wet by regular application of a drop of sterile phosphate-buffered saline (PBS). The nerves were sutured at both the proximal and distal anastomosis site with two 10-0 black filament sutures. The retracted muscles were placed back in position and the skin was sutured. All surgical manipulations were done under a microscope. Animals were transferred to a clean cage and allowed to recover under a heating lamp. Animals were carefully monitored for wound healing on a daily basis. Four weeks after transplantation, animals were sacrificed.

Perineurium permeability

A 1% Evans Blue (Sigma) solution in 5% bovine serum albumin (fraction V)/PBS (pH 7.4) was dialyzed overnight in PBS. The sciatic nerves of an adult claw paw animal and a wild-type littermate were dissected out and placed immediately in 4 ml of Evans blue albumin (EBA) solution at room temperature. After a 30- or 60-min incubation period, nerves were briefly washed in PBS and fixed in 4% paraformaldehyde for 2 h. Nerves were cryoprotected in 30% sucrose/PBS, frozen and sectioned at 24 μm. Sections were mounted in Vectashield® (Vector laboratories) and viewed immediately under a fluorescence microscope.

Quantitative RT-PCR

Total RNA was extracted from sciatic nerves using RNA-Bee (Tel Test Inc.). First-strand cDNA was generated using Superscript II (Invitrogen) reverse transcriptase and oligo-dT as primer. The following primers were used to amplify *dhh* and *cyclophilin* transcripts: dhh forward, CATGTGGC-

CCGGAGTACGCC; dhh reverse, CGCTGCATCAGCGGCCAGTA; cyclophilin forward, GGTCAACCCCACCGTGTTCTTCGACAT; cyclophilin reverse, GGACAAGATGCCAGGACCTGTATGCT. Annealing temperature for dhh primers: 60°C, annealing temperature for cyclophilin primers 68°C. Aliquots were taken from the reaction with two cycle intervals and amplification products were analyzed on a 1.8% agarose gel.

Light/electron microscopy

Anesthetized animals were sacrificed through transcardial perfusion with PBS (pH 7.4) for 3 min followed by fixative [3% PFA (Sigma); 1% glutaraldehyde (Sigma) in 100 mM cacodylate buffer, pH 7.2] for 10 min. Sciatic nerves were isolated, fixed overnight in the same fixative at 4°C. The next day, nerves were rinsed with 0.2 M cacodylate buffer, osmicated in 1% osmium tetroxide solution and embedded in Epon. Sections (1 μm) of Epon-embedded sciatic nerves were mounted on glass slides and stained with methylene blue. Ultra-thin cross sections from nerve grafts at mid-graft level were cut and uranyl acetate and lead citrate stained for electron microscopic analysis (Philips CM100).

Nerve conduction velocities

Nerve conduction velocities were measured on the tail nerve of anesthetized animals. Animals were placed on a thermo-comfort heating pad at 38°C. Recording and stimulation electrodes were made of 300-μm tungsten needles with a 10-μm tip. The stimulus frequency and stimulation period was 1 Hz and 0.1 ms, respectively. Impedance of the recording electrode was 100 and 25 kΩ/kHz for the stimulation electrode.

Immunohistochemistry

Rabbit polyclonal antibodies used in this study are directed against Oct-6 (Jaegle et al., 2003), Periaxin (Scherer et al., 1995) and Krox-20 (1:400). The Krox-20 antibody was raised against the unique amino-terminal portion of the protein (amino acids 1–180). Animals were immunized with 6xHis-tagged Krox-20^{1-180} protein expressed in *E. coli* (M15 strain) and purified on Ni^{2+}-NTA-agarose beads (QIAGEN). Mouse monoclonal antibodies used were against P-zero (1:1000) (Archelos et al., 1993) and neurofilament medium chain (1:200, hybridoma 2H3, Developmental Studies Hybridoma Bank).

Embryos and tissues were isolated, fixed in a mixture of methanol, acetone, acetic acid and water (35:35:5:25) for 1 h at 4°C, embedded in paraffin and sectioned at 7 μm. After dewaxing, tissue sections were hydrated and blocked in 1% BSA, 0.05% Tween-20 in PBS. Rabbit antibodies and mouse monoclonal antibodies were incubated simultaneously in PBS/0.05% Tween-20 overnight at room temperature. Oregon Green-conjugated goat anti-rabbit IgGs (Molecular Probes) and Texas Red-conjugated goat anti-mouse IgGs (Molecular Probes) were subsequently used as secondary antibodies. The tissue was viewed using a Leica fluorescence microscope.

Results

Morphological examination of clp nerves and comparison with Oct-6 mutant nerves

Our interest in the *clp* mouse mutant was initially raised by the similarities in peripheral nerve phenotypes between claw paw mice and *Oct-6* transcription factor mutant mice (Bermingham et al., 1996; Henry et al., 1991; Jaegle et al., 1996). Both mice are characterized by delayed initiation of myelination of their peripheral nerves. The similarities between these phenotypes suggested several possible interactions between the *Oct-6* and *clp* genes. For example, it is possible that the *clp* gene product is involved in those signaling pathways that activate *Oct-6* or, *clp* could be a major regulatory target of Oct-6. Alternatively, *clp* could act in a non-redundant pathway parallel to Oct-6. To begin to answer these questions, we first compared nerve morphology in both mutant and wild-type mice at several postnatal stages of development. Previously, nerve morphology in *clp/clp* animals has been described only from postnatal day 14 (P14) onwards (Henry et al., 1991). Therefore, we extended this analysis to include earlier stages of nerve development. Fig. 1 shows a comparison of representative transverse sections through the sciatic nerve of animals of different genetic background at different stages of postnatal development.

The sorting of prospectively myelinated axonal fibers by Schwann cells during late fetal development culminates in the promyelin stage of cell differentiation in which a Schwann cell has established a one to one relationship with its axon. These cells will exit the cell cycle, elaborate a basal lamina and initiate myelination. The majority of myelin-competent cells transit through this stage during the first week of postnatal life. This is evident in transverse section of the wild-type sciatic nerve at birth, in which many promyelin cells can be observed with some cells already actively myelinating (Fig. 1A, panel a). By P8, a majority of cells is actively myelinating and at P16 almost all myelin-competent cells are in an advanced stage of myelination (Fig. 1A, panels d and g). In contrast to wild-type, *clp/clp* Schwann cells are still at a very immature sorting stage at birth (Fig. 1, panel b). Most Schwann cells are found at the periphery of naked axon bundles, with cellular extensions pioneering into the bundles. This configuration of Schwann cells and naked axon bundles is typically observed in embryonic nerves around mouse embryonic day 17 (E17) (Feltri et al., 2002). To illustrate this developmental stage of *clp/clp* Schwann cells more graphically, we traced the

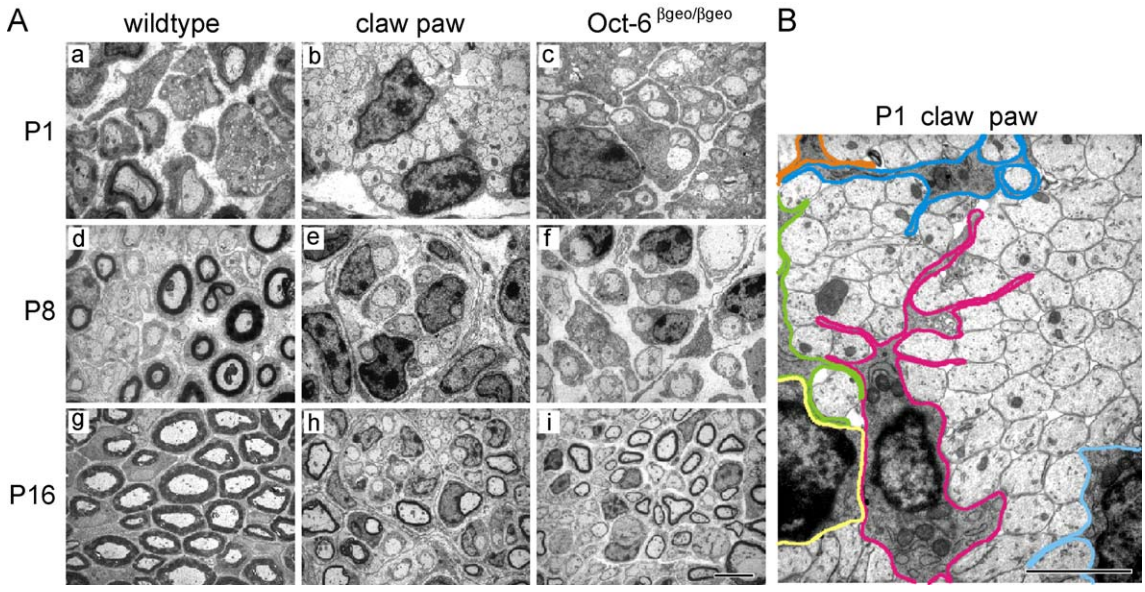

Fig. 1. Abnormal development of peripheral nerves in *clp/clp* and *Oct-6* mutant mice. (A) Shown are representative micrographs of transverse sections of sciatic nerves from wild-type, *clp/clp* (claw paw) and *Oct-6* mutant (Oct-6$^{\beta geo/\beta geo}$) animals at P1 (a, b and c), P8 (d, e and f) and P16 (g, h and i). At P1, axonal sorting is well advanced in wild-type nerves, with many axons in a 1:1 relationship with Schwann cells and few in an early myelinating stage (a). In contrast, axonal sorting in *clp/clp* nerves is in a very early stage with large groups of unsorted axons (b). Sorting in Oct-6 mutant nerves is well advanced with most cells in a late sorting and promyelin stage (c). At P8, the majority of myelin-competent Schwann cells in wild-type nerves are actively engaged in myelination (d), while in *clp/clp* nerves Schwann cells have now adopted a promyelin configuration (e). At this time, most Oct-6 mutant Schwann cells are still at the promyelin stage of differentiation (f). At P16, myelination is well advanced in wild-type nerves (g). In contrast, only a fraction of *clp/clp*, and Oct-6 mutant, Schwann cells have progressed to the myelinating stage of differentiation with many cells still at the promyelin stage (h and i). Scale bar: (a–c) 1.6 μm; (d–f) 2.8 μm; (g–i) 5 μm. (B) Axonal sorting is delayed in nerves of *clp/clp* (claw paw) mice. In this representative micrograph, *clp/clp* Schwann cells are just beginning to send out processes in the axon bundles. The outline of sorting Schwann cells is traced with a colored pencil. Each color represents an individual Schwann cell. Scale bar: 2 μm.

outline of several cells in a P1 nerve highlighting the cytoplasmic extensions of the sorting Schwann cell (Fig. 1B). One week later, these axon bundles are sorted out and a majority of Schwann cells have acquired a promyelin configuration (Fig. 1, panel e). Over the next week, many promyelin cells initiate myelination, such that by P16, a large number of myelin figures are observed. However, a substantial number of Schwann cells are still at the promyelin stage of cell differentiation, suggesting that this transition occurs at a lower rate in *clp/clp* Schwann cells than in wild-type Schwann cells (Fig. 1, panel h). By P32, the majority of *clp/clp* Schwann cells are actively meylinating with only few cells remaining in the promyelin configuration (data not shown and Henry et al., 1991). In contrast to *clp/clp* Schwann cells, *Oct-6* mutant Schwann cells transit through the sorting stage of development normally, but then stall at the promyelin stage for several days before initiating myelination (Fig. 1A, panels c, f and i). Thus, *clp/clp* Schwann cells appear strongly inhibited in the sorting stage of nerve development and to a lesser extent in the promyelinating to myelinating transition.

One other remarkable difference between *clp/clp* nerves and *Oct-6* mutant nerves (and wild-type nerves) is the extensive fasciculation of the former. Division of the endoneurium by flattened, perineurial-like cells is already apparent at P8 in *clp/clp* nerves (Fig. 1A, panel e). As illustrated in Fig. 2A, these cells contain, like perineurial sheath cells, many caveolae and secrete a basal lamina (arrows and arrowheads, respectively, in Fig. 2A, panel a). The number of cell layers that make up the perineurium and the morphology of the perineurial cells appear normal in *clp/clp* nerves at P16 and adult (Fig. 2A, panel b, and data not shown). The hyper-fasciculation phenotype observed in *clp/clp* peripheral nerves is reminiscent of that observed in *dhh* mutant animals (Parmantier et al., 1999). Therefore, it is possible that this particular aspect of the claw paw phenotype results from a failure to express *dhh* in the developing nerve. We therefore examined expression of *dhh* mRNA in *clp/clp* and wild-type nerves at P12 using quantitative PCR normalized to *cyclophilin* expression. We found that *dhh* is expressed in P12 *clp/clp* nerves, albeit at reduced levels (Fig. 2B). It is therefore possible that the extensive subdivision of *clp/clp* nerves by perineurial sheath cells is a consequence of reduced *dhh* expression. It has been hypothesized that the hyperfasciculation of *dhh* mutant nerves results from a functionally defective perineurium (Parmantier et al., 1999). A major function of the perineurium is to prevent the invasion of cells and macromolecules from the surrounding tissue into the endoneurium (Thomas et al., 1993). This nerve–tissue barrier function of the perineurium is compromised in *dhh* mutant animals as evidenced by the penetration of dye loaded serum albumin into the endoneu-

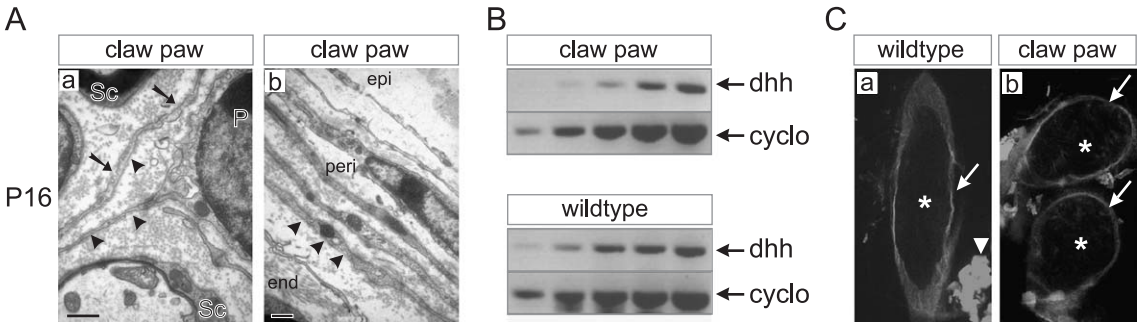

Fig. 2. Morphological and functional characterization of the perineurium of claw paw nerves. (A) Perineurial-like cells subdivide the endoneurium of claw paw nerves (panel a). This electron micrograph shows the typical flattened extensions of perineurial-like cells studded with numerous caveolae (arrows) and the basal lamina produced by these cells (arrowheads). Schwann cells (Sc) and the nucleus of a perineurial cell (P) are indicated. The number of cellular layers and the morphology of the perineurial cells appear normal in the developing perineurium of claw paw nerves (panel b). The epineurium is poorly defined at this stage and later stages. Scale bar: 500 nm. (B) *dhh* mRNA expression is reduced in claw paw nerves. Expression levels of *dhh* were estimated using quantitative RT-PCR during the exponential phase of the reaction and normalized against cyclophilin (cyclo), a housekeeping gene expressed at rather constant levels. Samples were taken with two-cycle intervals. It is estimated that *dhh* mRNA levels are 4- to 16-fold lower in claw paw nerves at P12. (C) The nerve–tissue barrier function of the perineurium is intact in claw paw nerves. Following submersion of dissected sciatic nerve of wild-type (panel a) or claw paw nerve (panel b) for 1 h in EBA solution, EBA is found associated with the epi- and perineurial sheath of the nerve (arrows). EBA did not penetrate the endoneurium of wild-type or claw paw nerves (asterisk). However, strong EBA staining is seen within muscle tissue lying next to the nerve (arrowhead).

rium (Parmantier et al., 1999). We similarly tested the integrity of the tissue–nerve barrier in claw paw nerves. After 1 h exposure to a Evans blue albumin solution ex vivo, nerves were processed for fluorescence microscopy. No dye complex had penetrated the endoneurium of wild-type or claw paw nerves (Fig. 2C, panels a and b, respectively) demonstrating that, in contrast with *dhh* mutant nerves, the nerve–tissue barrier in claw paw mice is intact. Thus, *clp/clp* nerves resemble *dhh* mutant nerves in their extensive subdivision into smaller fascicles by perineurial sheath cells but have, unlike *dhh* mutant nerves, a functionally intact perineurium.

Activation of Oct-6 expression in clp/clp nerves

As previous work has demonstrated that the transcription factors Oct-6 and Krox20 are major cell-autonomous regulators of the Schwann cell myelination program, it is possible that the delayed myelination phenotype in *clp/clp* nerves can in part be explained by a failure to activate Oct-6 and subsequently Krox-20, in *clp/clp* animals (Ghislain et al., 2002). We therefore examined expression of Oct-6, Krox-20 and the myelin proteins P-zero and periaxin in *clp/clp* animals at P8 and P16 by immunohistochemistry and compared it with the expression of these proteins in wild-type and *Oct-6* mutant Schwann cells (Fig. 3). At P8, most *clp/clp* Schwann cells are, like most *Oct-6* mutant cells, at the promyelin stage of cell differentiation (see Fig. 1) and will commence myelination in the course of the next 2 weeks. As shown in Fig. 3A, Oct-6 is expressed in Schwann cells of *clp/clp* animals at P8. This is in agreement with previous mRNA expression data (Bermingham et al., 2002). As reported earlier, Oct-6 is an upstream regulator of Krox-20 and hence, *Oct-6* mutant Schwann cells do not express Krox-20 (Ghazvini et al., 2002; Ghislain et al., 2002). Despite the expression of Oct-6 in *clp/clp* Schwann cells, Krox-20 is not expressed at P8, but eventually is activated in *clp/clp* nerves (and *Oct-6* mutant nerves) when myelination proceeds (Ghazvini et al., 2002 and Fig. 3B, panel a). As expected, P-zero expression is very low in both mutant mouse strains at P8, as the majority of Schwann cells have not yet produced compact myelin (Fig. 3A, panels h and i). However, at P16, *clp/clp* nerves show strong P-zero immunoreactivity in myelin-forming Schwann cells (Fig. 3B, panel b). Interestingly, the myelin protein periaxin appears reduced or misexpressed in *clp/clp* Schwann cells at P8. This is in contrast to promyelin-arrested *Oct-6* mutant Schwann cells in which periaxin is expressed at near normal levels (panels j, k and j). However, once *clp/clp* cells form compact myelin, high levels of periaxin are observed in these cells (Fig. 3B, panel c). Thus, in contrast to *Oct-6* mutant Schwann cells, periaxin protein does not accumulate in promyelin-arrested *clp/clp* Schwann cells suggesting that the *clp* mutation affects activation of periaxin expression or subcellular localization and/or processing.

To distinguish between these possibilities, we further examined periaxin expression at late fetal stages of development in *clp/clp* and wild-type animals. Periaxin is first expressed in the nuclei of embryonic Schwann cells at E14. By E17, periaxin expression shifts to the cell membrane and by E18, periaxin is no longer found in the nucleus (Sherman and Brophy, 2000). We examined periaxin expression in *clp/clp* Schwann cells of embryonic nerves at E17, the stage at which claw paw animals can first be recognized. No periaxin is detected in *clp/clp* nerves at this stage (Fig. 4A, panel d). In contrast, wild-type Schwann cells express periaxin in the nucleus and/or in the cytoplasm (Fig. 4A, panel c). Thus, the *clp* mutation affects onset of periaxin expression at this embryonic stage and subsequently, also the subcellular localization of the periaxin protein.

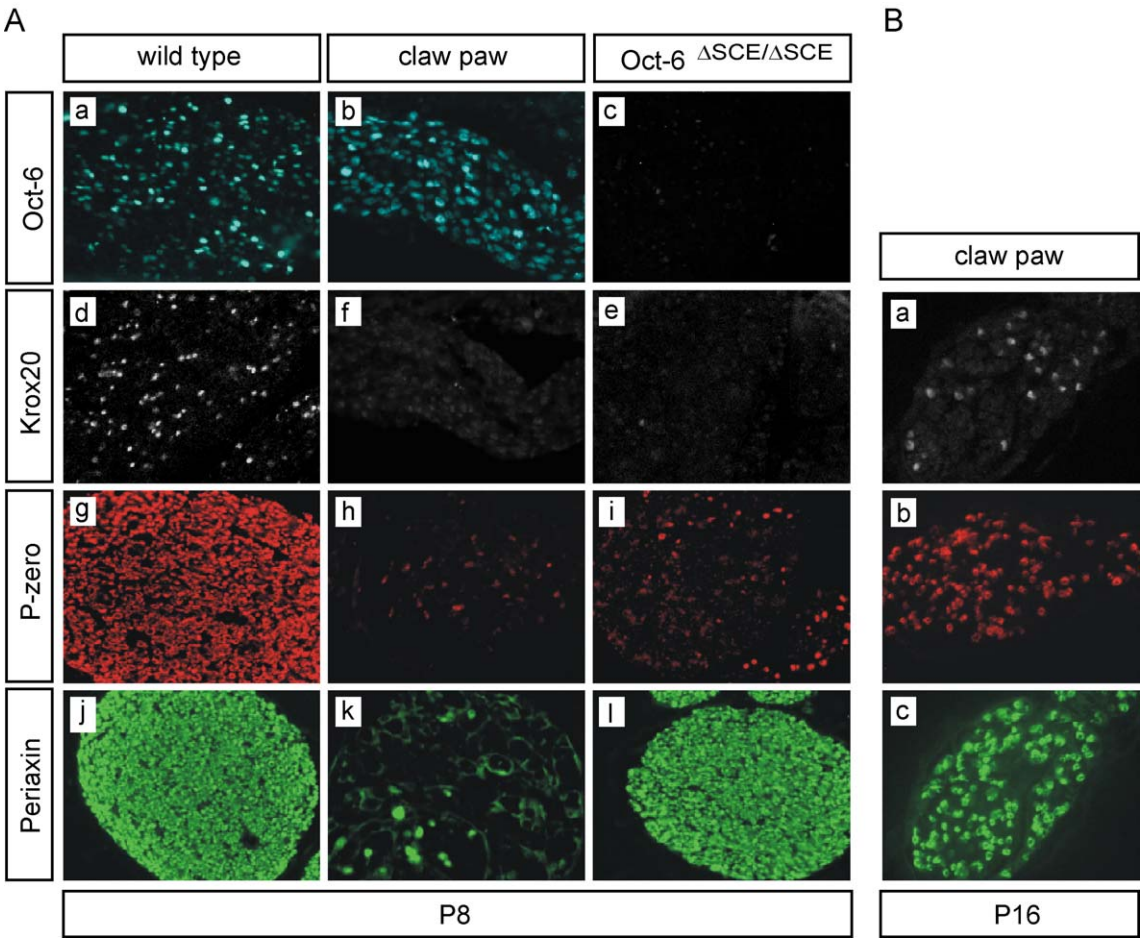

Fig. 3. Developmental expression of Oct-6, Krox-20, P-zero and periaxin in *clp/clp* and *Oct-6* mutant nerves. (A) Transverse sections of sciatic nerves of *clp/clp* (claw paw), *Oct-6* mutant (Oct-6$^{\Delta SCE/\Delta SCE}$) and control (wild-type) mice at P8 were stained for Oct-6 (a–c), Krox-20 (d–e), P-zero (g–i) and periaxin (j–l). In the control nerve, myelinating Schwann cells express Oct-6, Krox-20 and the myelin proteins P-zero and periaxin (a, d, g and j). At P8, most *clp/clp* Schwann cells have adopted a promyelin configuration and express Oct-6 (b) but not the myelination-associated transcription factor Krox-20 (f). Some cells express appreciable levels of P-zero. These cells are probably in an advanced promyelin stage as there is no evidence of compact myelin yet at this stage (h). Very low cytoplasmic periaxin expression is observed in many, but not all, cells (k). Few cells exhibit high level of periaxin expression. No nuclear periaxin staining is observed at this stage. Like *clp/clp* Schwann cells, *Oct-6* mutant Schwann cells do not express Oct-6 or Krox-20 at this stage (c and e). The few cells that have initiated myelin formation are strongly positive for P-zero (i). In strong contrast to *clp/clp* Schwann cells (k), *Oct-6* mutant cells express already high levels of periaxin at this stage (l). Magnification ×40. (B) Myelin formation is evident in *clp/clp* nerves at P16. An appreciable number of Schwann cells have initiated myelination and express Krox-20 (a). High levels of P-zero and periaxin are present in Schwann cells that have formed compact myelin (b and c). Magnification ×40.

We next examined whether Oct-6 is also delayed in its onset of expression. Oct-6 protein normally starts to accumulate in the nuclei of immature Schwann cells of the sciatic nerve at late fetal stages and reaches maximum levels in promyelin cells during the first postnatal week of development. As *clp/clp* Schwann cells at P1 morphologically resemble Schwann cells in E16–E17 wild-type embryonic nerves, we examined Oct-6 expression in P1 *clp/clp* nerves. At this stage, we found that *clp/clp* Schwann cells already express appreciable levels of Oct-6 (Fig. 4B, panel b), demonstrating that the clp gene product does not affect activation of Oct-6 expression. In contrast to wild-type Oct-6-positive Schwann cells, Oct-6-positive *clp/clp* Schwann cells do not express appreciable levels of P-zero protein (Fig. 4B, panels c and d).

Taken together, these data demonstrate that the *clp* mutation affects nerve maturation through a pathway that includes activation of periaxin, but not Oct-6, and thus strongly suggest that during Schwann cell differentiation, periaxin and Oct-6 are regulated through distinct signaling pathways.

Nerve conduction velocities of clp nerves are reduced

The delayed maturation of peripheral nerves in *clp/clp* animals results in reduced internodal lengths for all diameter classes and thus, in the absence of axonal loss, increased Schwann cell numbers. In addition, myelin thickness is reduced in some, but not all, *clp/clp* animals and no decrease in mean axon diameter was reported (Henry et al., 1991;

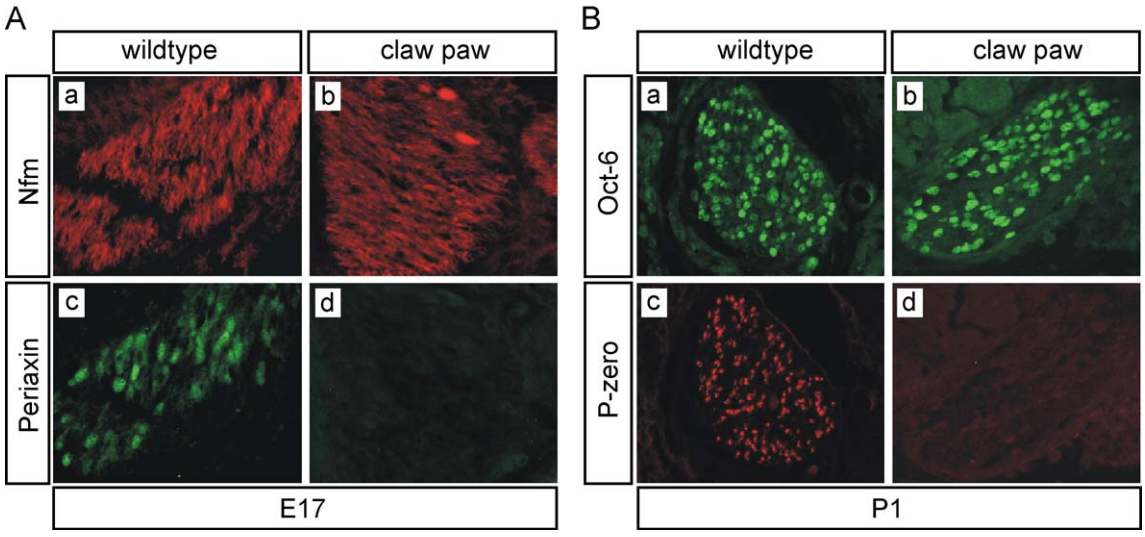

Fig. 4. Expression of periaxin and Oct-6 in *clp/clp* Schwann cells. (A) Embryonic sciatic nerve is visualized by expression of the neurofilament medium chain in the axonal fibers (Nfm; a and b). Embryonic Schwann cells within the nerve express periaxin in their cytoplasm or nucleus (c). In contrast, no periaxin expression is observed in nerves of claw paw embryos at this stage of development (d). (B) Oct-6 is expressed in all Schwann cells in newborn wild-type sciatic nerves (a). Also, Schwann cells in sciatic nerves of *clp/clp* animals express Oct-6 (b). Other than wild-type Schwann cells, *clp/clp* Schwann cells uniformly express high levels of Oct-6. In wild-type nerves, many Schwann cells are at the promyelin configuration and some have initiated myelination and thus express high levels of P-zero (c). In contrast, *clp/clp* Schwann cells appear at an early sorting stage at P1 (see Fig. 1) and do not express detectable levels of P-zero protein (d).

Koszowski et al., 1998). The mean internodal length in every axonal diameter class in *clp/clp* animals is approximately half of that of wild-type animals. Intuitively, and on theoretical considerations, it is to be expected that propagation of action potentials will be slowed when the mean internodal length drops well below its optimum (Brill et al., 1977; Goldman and Albus, 1968; Rushton, 1951). To assess nerve conduction velocity (NCV) in *clp* and wild-type animals, we measured compound action potentials (CAP) of the tail nerve (Fig. 5A). The mean NCV in wild-type and heterozygous mice was 35.3 m/s (SD 1.8). In contrast, the mean NCV in *clp/clp* mice was 23.9 m/s (SD 2.2), a reduction of 35% (Fig. 5B). A similarly reduced conduction velocity was observed for motor nerves within the sciatic nerve of *clp/clp* animals as compared to wild type (data not shown). Reduced NCV in the tail nerve of claw paw mice shows little variance, and this variance does not correlate with age or severity of the behavioral phenotype. Thus, it is possible that the reduction in NCV in *clp/clp* animals can be accounted for, at least in part, by the reduction in mean internodal length.

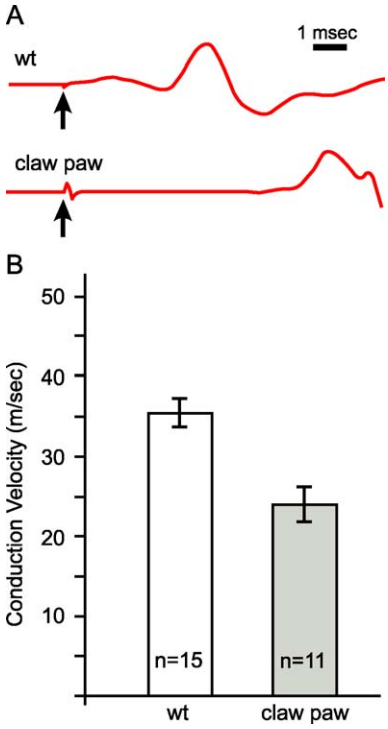

Fig. 5. Nerve conduction velocities are reduced in *clp/clp* nerves. (A) Representative recordings of compound action potentials of the tail nerve of wild-type (wt) and *clp/clp* (claw paw) animals. Arrows indicate the stimulation artefact. (B) Mean conduction velocity for wild-type (wt) and *clp/clp* (claw paw) nerves. The number (*n*) of animals from which recordings were obtained in each group is indicated. The error bar represents standard deviation. The difference in mean NCV between *clp/clp* and wild-type animals is significant ($P < 0.00001$, Student's *t* test).

Response to nerve injury

Although the claw paw phenotype has been described as a developmental abnormality, it is not clear from these observations whether the phenotype results from an intrinsic defect in one or more components of the developing nerve or through defects in other organs of the developing fetus. Studying the damage response of the nerve in the adult animal allows examination of Schwann cell–axon interac-

tions that are largely a reiteration of developmental events (Scherer and Salzer, 1996). Following nerve transection, axons and myelin in the distal nerve segment disintegrate in a process called Wallerian degeneration. Schwann cells revert back to an immature pre-myelinating phenotype, proliferate and participate with macrophages in the removal of myelin and axonal debris. These reactive Schwann cells create an environment that stimulates axonal regeneration of the transected neurones. Upon restoration of axonal contact, Schwann cells differentiate into myelin or non-myelin forming cells (Scherer and Salzer, 1996). Therefore, if the *clp* defect resides within the nerve tissue, it is likely that at least part of the defect will be recapitulated during nerve regeneration following nerve axotomy in an adult animal. On the other hand, if the *clp* defect is strictly developmental and not intrinsic to the nerve tissue, it is expected that regeneration will be relatively normal.

To examine the effect of the *clp* mutation on Schwann cell–axon interaction during regeneration, the sciatic nerve of adult *clp/clp* and wild-type mice were crushed and studied morphologically 4 weeks later (Fig. 6). The nerves were sectioned at two levels distal to the injury, 3 and 6 mm, respectively, representing two successive stages of regeneration. In wild-type animals, regeneration is well advanced, with only few remnants of myelin remaining (arrows in Fig. 6A, panel b) and most axons associated with compact myelin. Regeneration of *clp/clp* nerves differs significantly from wild-type nerves in some aspects. First, most large-caliber axons are ensheathed by a single Schwann cell, but only a few of these are associated with a thin compact myelin sheath (Fig. 6A, panels e and f). Second, supernumerary Schwann cells surround large axon–Schwann cell units and are associated with numerous thin axons (Fig. 6B). These structures are enclosed by the original basal lamina (arrows in Fig. 6B), indicating excessive sprouting of the regenerating axon. Third, excessive fasciculation results in a further subdivision of the *clp* nerve (Fig. 6A, panels e and f). Thus, while *clp* axons do grow back into the distal nerve stump, regeneration is clearly disturbed. Some of these regeneration abnormalities, such as delayed myelination and hyper-fasciculation, are also observed during development suggesting that the *clp* defects are caused by a nerve intrinsic defect in one or more components within the developing or regenerating nerve.

Nerve grafting

To distinguish between a Schwann cell and neuronal defect in the regeneration of *clp/clp* nerves, we performed nerve grafting experiments. Nerve transplantation experiments create a situation in which Schwann cells, genetically distinct from the host, differentiate in association with host-derived neurons (Aguayo et al., 1977; de Waegh and Brady, 1991; Scaravilli and Jacobs, 1981). We performed nerve transplantation operations in which a wild-type host was engrafted with a segment of a wild-type (wt:wt) or *clp/clp* (clp:wt) sciatic nerve segment. Also, the converse set of transplantations was performed in which a *clp/clp* host was engrafted with a wild-type (wt:clp) or *clp/clp* (clp:clp) sciatic nerve segment. The poorly developed epineurium of *clp/clp* nerves as compared to that of wild-type nerves made the grafting of the segments particularly demanding on the technical level. Four weeks after the operation, the transplanted nerves were isolated and examined microscopically. Each nerve was serially sectioned and examined at 250-μm intervals. Representative sections from the middle of the graft and proximal and distal to the anastomosis site are shown in Fig. 7. In the wt:wt transplantation, regenerat-

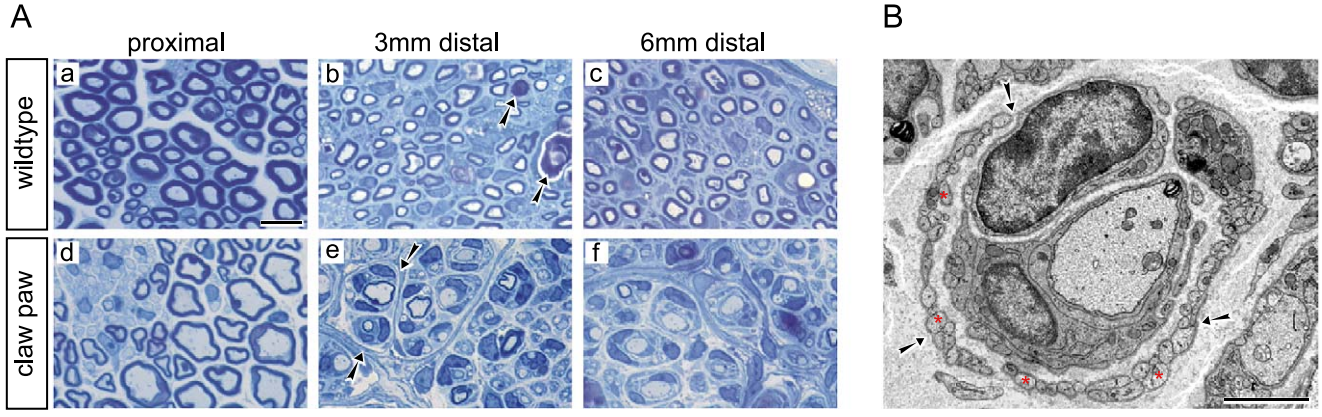

Fig. 6. Abnormal response to nerve injury in *clp/clp* mice. (A) Light micrographs of cross sections of sciatic nerves of young adult wild-type and *clp/clp* (claw paw) animals 4 weeks after nerve crush. The myelin sheath in *clp/clp* nerves is thinner than in wild-type nerves, as described earlier (a and d). In wild-type nerves, regeneration is well advanced, both at 3 and 6 mm distal of the nerve crush (b and c), with only little myelin debris remaining (arrows in panel b). All regenerated axons are myelinated. Regeneration in *clp/clp* nerves is delayed with only few regenerated axons myelinated. This is even more pronounced at 6 mm distal to the lesion, corresponding to a later time point in regeneration (f). Excessive fasciculation is evident in the regenerating nerve. A layer of epineural cells enclosing a group of regenerating fibers is indicated with arrows (e). Scale bar: 10 μm. (B) In this electron micrograph of a regenerating *clp/clp* nerve, supernumerary Schwann cells are associated with regenerating axons. In addition to the large central axon, excessive numbers of axon sprouts (red asterisks) are observed within the regenerating unit that is enclosed by one basal lamina (arrows). The cross section is through three Schwann cells. Scale bar: 2 μm.

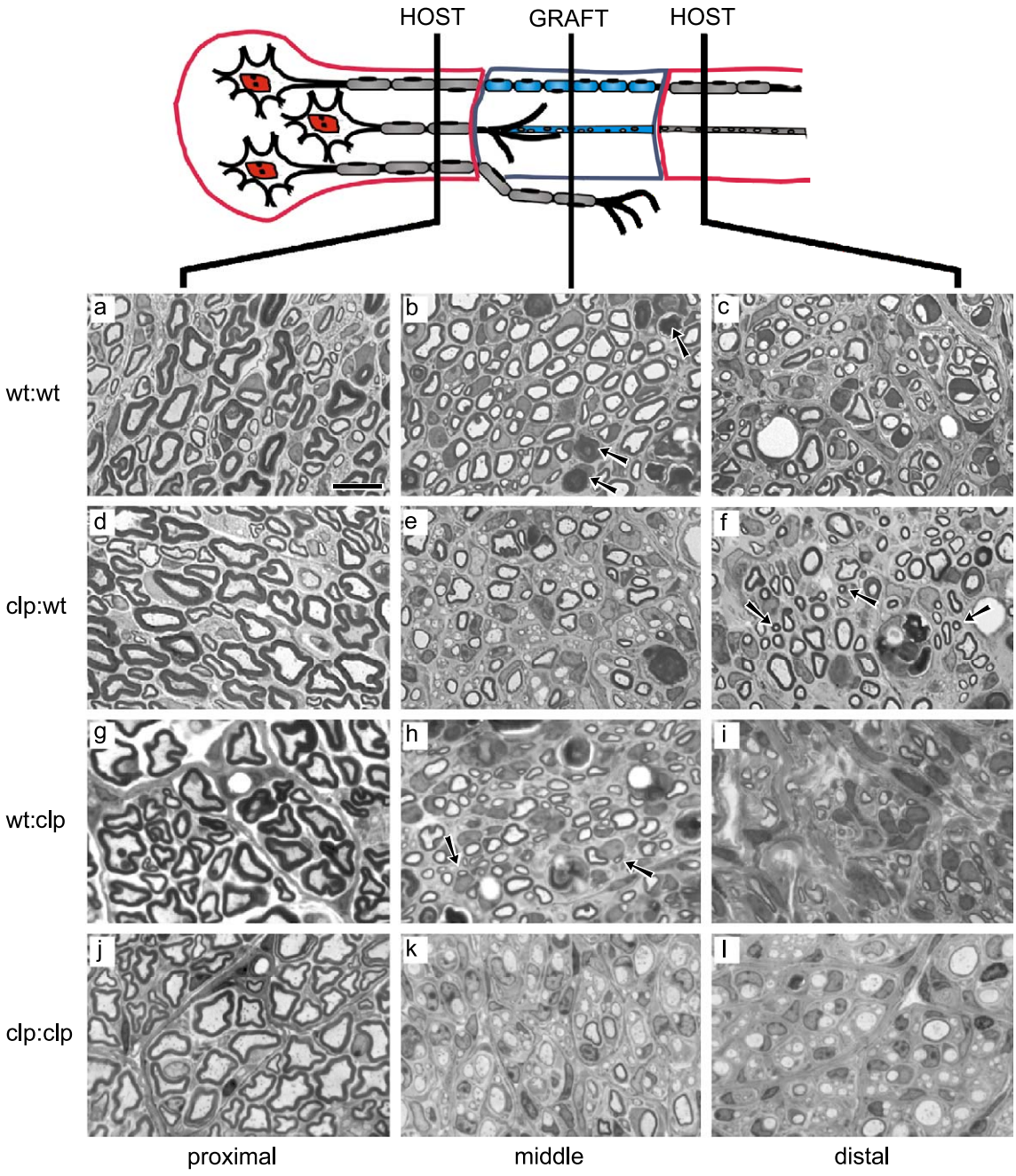

Fig. 7. Nerve grafting experiments reveal Schwann cell and neuronal expression of the *clp* defect. Light micrographs of semi-thin cross sections of sciatic nerve at three different levels of the engrafted nerve 4 weeks after the operation. The position of the sections relative to the engrafted segment is schematically depicted in the diagram above the micrographs. At the level of the engrafted segment and distal to this segment, three different configurations are expected: regenerated axons myelinated by graft-derived Schwann cells (blue in diagram); Schwann cell tubes (blue) that do not get re-innervated by host neurones and host axons that do not enter the nerve graft and are associated with host-derived Schwann cells (gray in diagram) that migrate with the regenerating axons. Donor and recipient genotypes (donor/recipient) are listed to the left. Non-innervated Schwann cell tubes with myelin debris are indicated with arrows in panel b. Thinly myelinated axons that have re-innervated the distal nerve segment of the wild-type host are indicated in panel f with arrows. Arrows in panel h also point to regenerating wild-type axons that are myelinated by *clp/clp* Schwann cells. For further details, see text. Scale bar: 10 μm.

ing axons have grown through the graft and entered the distal nerve stump. Wild-type Schwann cells in the graft and distal nerve stump have formed compact myelin around regenerated axons (Fig. 7, panels b and c). Schwann cell tubes (reactive Schwann cells within their basal lamina: bands of Bunger) that were not re-innervated still contain some myelin debris (arrows in panel b). In the clp:wt transplantation, wild-type axons do regenerate through a *clp/clp* nerve graft into the distal nerve stump (Fig. 7, panels e and f). Moreover, in contrast to wild-type Schwann cells, *clp/clp* Schwann cells have only myelinated the larger axons in the graft and many axons are still in an early ensheathing

or promyelin configuration (panel e). Smaller axons that have navigated through the graft and have entered the distal nerve stump are normally myelinated (arrows in panel f). These observations suggest that at least part of the delayed myelination phenotype in *clp/clp* animals is Schwann cell autonomous.

Transplantations of wild-type nerve segments into *clp/clp* hosts were less successful as ligations to the distal nerve stump did not hold. Nevertheless, *clp/clp* axons did enter the wild-type nerve graft and were myelinated by the wild-type Schwann cells within the graft (Fig. 7, panel h). Also smaller-caliber claw paw axons were myelinated (arrows in panel h). Distal to the second anastomosis site, regrowing axons did not enter the distal nerve stump, but were found associated with a large blood vessel (not shown). Most likely, graft-derived perineural cells and Schwann cells accompany these axons (panel i). Notwithstanding, these data suggest that wild-type Schwann cells receive appropriate signals from *clp/clp* neurones to myelinate them. Finally, the clp:clp transplantations show that *clp/clp* axons do grow through the grafted segment into the distal nerve stump. Consistent with the results in the *clp/clp* nerve crush experiment (Fig. 6), regenerating *clp/clp* axons are associated with supernumerary Schwann cells and only few axons are thinly myelinated (Fig. 7, panels k and l). We also observe a further increase in the extent of fasciculation. This increased fasciculation was less pronounced in the clp:wt and in wt:clp transplantations. Therefore, this specific aspect of the claw paw phenotype arises mainly from interaction of *clp/clp* axons with the *clp/clp* endoneurium. This is also true for the delayed myelination phenotype, as it is much more severe in the clp:clp transplantation than in the clp:wt and wt:clp transplantations. Thus, while the former two grafting experiments (wt:clp and clp:wt) suggest a Schwann cell autonomous effect of the *clp* mutation on myelination, the nerve crush and clp:clp transplantation suggest that there is also an important Schwann cell non-autonomous, most likely neuronal, aspect to the *clp* mutation.

Discussion

We have studied the cellular and molecular basis of the congenital limb abnormality manifested by claw paw mutant mice. Our findings demonstrate that the *clp* mutation affects both the axonal and endoneural/Schwann cell compartment, resulting in axonal sorting and myelination defects. At the molecular level, *clp* affects a signaling pathway that is parallel and non-redundant to the Oct-6-dependent pathway, suggesting that axonal signals that drive Schwann cell differentiation and myelination are transduced through multiple parallel pathways. These findings suggest several possible roles for the *clp* gene and, additionally, define a set of requirements for *clp* candidate genes, to be identified in the ongoing positional cloning effort.

What process in nerve development is affected by the clp mutation?

The development of peripheral nerve tissue can be conveniently thought of as an ordered series of cellular transitions that result from several complex interactions between Schwann cells, axons, mesenchymal cells and extracellular components (Jessen and Mirsky, 1999; Webster, 1993). The first transition occurs when migrating neural crest cells associate with outgrowing axon bundles and acquire Schwann cell precursor characteristics (Jessen and Mirsky, 1991; Jessen et al., 1994). These cells proliferate, migrate with the growing axons and, in a second transition, differentiate into immature Schwann cells that invade the axon bundles and start the process of radial sorting of nerve fibers. This process culminates in larger axons singled out by individual Schwann cells (promyelin stage) which, in a third transition, will go on to myelinate their axon and multiple smaller axons associated with Schwann cells to form the so-called Remak fibers of non-myelinated axons. During this last phase, immature Schwann cells exit the cell cycle and elaborate an extracellular matrix. The peri- and epineural layers that surround and protect the nerve differentiate from the surrounding mesenchyme in a process that requires Schwann cell-derived desert hedgehog signaling (Bunge et al., 1989; Du Plessis et al., 1996; Parmantier et al., 1999).

The major defects in the developing and adult peripheral nerves of claw paw mutant mice were originally described as a general delay of myelination initiation and the persistence of promyelin fibers in adult animals (Henry et al., 1991). On the basis of these morphological observations, Henry et al. hypothesized that the *clp* defect affects the complex signaling between axon, Schwann cell and extracellular components that control the transition of promyelin Schwann cells into myelinating cells. Molecular studies have shown that this transition is mediated by the activity of the transcription factors Oct-6 and Krox-20 acting consecutively in the Schwann cells (Ghislain et al., 2002). Our finding that *clp* does not affect activation of Oct-6 expression but that Krox-20 activation is delayed suggests that *clp* acts either downstream of Oct-6 or in a second non-redundant pathway.

Several observations presented here argue in favor of the second possibility. Morphological examination of nerves of newborn claw paw animals revealed that Schwann cells are still at an early sorting stage of development while wild-type and *Oct-6* mutant Schwann cells are at the end of the sorting stage. This early sorting stage observed in P1 *clp/clp* nerves would be appropriate for embryonic nerves in E16–E18 wild-type embryos. Sorting and ensheathment of axons by Schwann cells critically depends on rearrangements of the Schwann cell cytoskeleton. Deletion of the β1 integrin or the laminin γ1 gene in Schwann cells results in impaired sorting of axon bundles, suggesting that these rearrangements are mediated through interactions between the extracellular matrix laminins and their integrin receptors (Chen

and Strickland, 2003; Feltri et al., 2002; Saito et al., 2003). The similarity in ultrastructural abnormalities observed in newborn *clp/clp*, β1 integrin and laminin γ1 mutant nerves, suggests that clp acts in these pathways. In contrast to laminin γ1 null Schwann cells, *clp/clp* Schwann cells are not permanently blocked at the sorting stage. It is therefore likely that a *clp* redundant function exists or that the *clp* allele is a hypomorph.

In addition, *clp/clp* nerves exhibit hyperfasciculation, a phenotype resembling that observed in *dhh* mutant mice, suggesting the possibility that this specific aspect of the claw paw mutant phenotype results from downregulation of dhh expression. In agreement with this suggestion, we found that *dhh* mRNA is expressed at reduced levels in *clp/clp* nerves (at P12). However, in contrast to *dhh* mutant animals, the nerve–tissue barrier function of the perineurium in claw paw animals is not affected (Fig. 2). As the biological effects of hedgehog proteins are known to be dose-dependent, it is tempting to speculate that the differences in phenotype between *dhh* mutant and *clp/clp* nerves reflect differences in *dhh* expression levels in the developing nerves of these two mutant animals.

Nuclear periaxin expression in embryonic Schwann cells, and the later accumulation of periaxin in promyelin cells at P8, is not observed in claw paw nerves at these stages (Figs. 2 and 3), although periaxin does eventually accumulate in Oct-6 and Krox-20 expressing myelinating *clp/clp* Schwann cells (Fig. 2). It has recently been suggested that a dual mechanism of periaxin regulation exists in which Krox-20 amplifies an earlier Krox-20 independent activation of the periaxin gene (Parkinson et al., 2003). Our results suggest further that the early Krox-20 independent activation of periaxin is regulated through a *clp*-dependent pathway. Alternatively, it is possible that *clp* Schwann cells at E17 represent an earlier differentiation stage at which periaxin is not expressed yet (they will have to be very early Schwann cell precursors, as E14 Schwann cell precursors express periaxin in their nuclei, (Sherman and Brophy, 2000). It is unlikely that the absence of detectable levels of periaxin in *clp* Schwann cells contributes significantly to the peripheral nerve phenotype in claw paw mice, as peripheral nerve development is morphologically normal in *periaxin* null mice (Gillespie et al., 2000).

Thus, in contrast to what has been suggested earlier, the *clp* mutation affects nerve development at a stage well before the promyelin-myelinating transition. The particular defects suggest that *clp* is involved in axon–Schwann cell interactions that drive the invasion and sorting of immature Schwann cells and the subsequent elaboration of a basal lamina and myelination initiation.

On the nature of the claw paw mutation

In the absence of knowledge about the mutation underlying the claw paw phenotype, we do not know what mechanism could account for the peripheral nerve developmental defect and the behavioral defect in claw paw animals. However, on the basis of the observed developmental defects, the recessive nature of the *clp* mutation and in particular the results of regeneration and nerve transplantation experiments, we can speculate on possible scenarios. Although the morphological abnormalities observed in the nerve of claw paw animals suggest that the *clp* mutation affects primarily Schwann cells, the transplantation and nerve regeneration experiments suggest that *clp* function might also be required in the neurone and possibly the endoneurial fibroblasts. It is therefore likely that the *clp* gene product is expressed and functioning in both Schwann cells and neurones and that the *clp* mutation is not a gain of function mutation. These suggestions are compatible with *clp* functioning in, or regulating, homo- or heterophilic interactions between axons and Schwann cells. For example, it is possible that the claw paw protein is involved in bringing adhesion molecules to the cell surface or that claw paw itself is a cell surface protein directly involved in cell–cell interactions. Alternatively, it is possible that the *clp* mutation is a regulatory mutation affecting expression of genes involved in the abovementioned interactions. These impaired axon Schwann cell interactions at an early stage could have repercussions for nerve activity during fetal stages and affect the normal spontaneous movement of the fetus, important for proper posture development.

In summary, we have provided evidence that the mouse *clp* mutation affects the Schwann cell compartment and possibly the neuronal compartment of the regenerating and, by extension, the developing nerve, suggesting that the *clp* gene is expressed in Schwann cells and neurones and is involved in direct axon–Schwann cell interactions. Furthermore, the *clp* mutation affects early activation of periaxin expression and Krox20 expression in Schwann cells, but does not affect the signaling pathway that activates Oct-6 expression, suggesting that axonal signals that initiate myelination are transduced through multiple parallel, non-redundant pathways.

Acknowledgments

We thank Elaine Dzierzak and Sjaak Philipsen for their comments and encouragement. Thanks also to Peter Brophy and Juan Archelos who provided the periaxin antibody and the P-zero antibody, respectively. All animal work was performed according to institutional and European guidelines and approved by the animal experimentation review board (DEC). This work was supported in part by grants from the Dutch Research Council NWO (MW-901-01-205 and 903-42-195).

References

Aguayo, A.J., Attiwell, M., Trecarten, J., Perkins, S., Bray, G.M., 1977. Abnormal myelination in transplanted Trembler mouse Schwann cells. Nature 265, 73–75.

Archelos, J.J., Roggenbuck, K., Schneider-Schaulies, J., Linington, C., Toyka, K.V., Hartung, H.P., 1993. Production and characterization of monoclonal antibodies to the extracellular domain of P0. J. Neurosci. Res. 35, 46–53.

Bermingham, J.R., Scherer, S.S., Oconnell, S., Arroyo, E., Kalla, K.A., Powell, F.L., Rosenfeld, M.G., 1996. Tst-1/Oct-6/SCIP regulates a unique step in peripheral myelination and is required for normal respiration. Genes Dev. 10, 1751–1762.

Bermingham Jr., J.R., Shumas, S., Whisenhunt, T., Sirkowski, E.E., O'Connell, S., Scherer, S.S., Rosenfeld, M.G., 2002. Identification of genes that are downregulated in the absence of the POU domain transcription factor pou3f1 (Oct-6, Tst-1, SCIP) in sciatic nerve. J. Neurosci. 22, 10217–10231.

Boylan, K.B., Ferriero, D.M., Greco, C.M., Sheldon, R.A., Dew, M., 1992. Congenital hypomyelination neuropathy with arthrogryposis multiplex congenita. Ann. Neurol. 31, 337–340.

Brill, M.H., Waxman, S.G., Moore, J.W., Joyner, R.W., 1977. Conduction velocity and spike configuration in myelinated fibres: computed dependence on internode distance. J. Neurol., Neurosurg. Psychiatry 40, 769–774.

Bunge, M.B., Wood, P.M., Tynan, L.B., Bates, M.L., Sanes, J.R., 1989. Perineurium originates from fibroblasts: demonstration in vitro with a retroviral marker. Science 243, 229–231.

Charnas, L., Trapp, B., Griffin, J., 1988. Congenital absence of peripheral myelin: abnormal Schwann cell development causes lethal arthrogryposis multiplex congenita. Neurology 38, 966–974.

Chen, Z.L., Strickland, S., 2003. Laminin gamma1 is critical for Schwann cell differentiation, axon myelination, and regeneration in the peripheral nerve. J. Cell Biol. 163, 889–899.

de Waegh, S.M., Brady, S.T., 1991. Local control of axonal properties by Schwann cells: neurofilaments and axonal transport in homologous and heterologous nerve grafts. J. Neurosci. Res. 30, 201–212.

Del Torto, U., Bianchi, O., Pone, G., Sante, G., 1983. Experimental study on the etiology of congenital multiple arthrogryposis. Ital. J. Orthop. Traumatol. 9, 91–99.

Drachman, D.B., 1971. The syndrome of arthrogryposis multiplex congenita. Birth Defects, Orig. Artic. Ser. 7, 90–97.

Drachman, D.B., Coulombre, A.J., 1962. Experimental clubfoot and arthrogryposis multiplex congenita. Lancet 15, 523–526.

Du Plessis, D.G., Mouton, Y.M., Muller, C.J., Geiger, D.H., 1996. An ultrastructural study of the development of the chicken perineurial sheath. J. Anat. 189, 631–641.

Feltri, M.L., Graus Porta, D., Previtali, S.C., Nodari, A., Migliavacca, B., Cassetti, A., Littlewood-Evans, A., Reichardt, L.F., Messing, A., Quattrini, A., Mueller, U., Wrabetz, L., 2002. Conditional disruption of beta 1 integrin in Schwann cells impedes interactions with axons. J. Cell Biol. 156, 199–209.

Fields, R.D., Stevens-Graham, B., 2002. New insights into neuron–glia communication. Science 298, 556–562.

Ghazvini, M., Mandemakers, W., Jaegle, M., Piirsoo, M., Driegen, S., Koutsourakis, M., Smit, X., Grosveld, F., Meijer, D., 2002. A cell type-specific allele of the POU gene Oct-6 reveals Schwann cell autonomous function in nerve development and regeneration. EMBO J. 21, 4612–4620.

Ghislain, J., Desmarquet-Trin-Dinh, C., Jaegle, M., Meijer, D., Charnay, P., Frain, M., 2002. Characterisation of cis-acting sequences reveals a biphasic, axon-dependent regulation of Krox20 during Schwann cell development. Development 129, 155–166.

Gillespie, C.S., Sherman, D.L., Fleetwood-Walker, S.M., Cottrell, D.F., Tait, S., Garry, E.M., Wallace, V.C., Ure, J., Griffiths, I.R., Smith, A., Brophy, P.J., 2000. Peripheral demyelination and neuropathic pain behavior in periaxin-deficient mice. Neuron 26, 523–531.

Goldman, L., Albus, J.S., 1968. Computation of impulse conduction in myelinated fibers; theoretical basis of the velocity–diameter relation. Biophys. J. 8, 596–607.

Hageman, G., Willemse, J., 1983. Arthrogryposis multiplex congenita. Neuropediatrics 14, 6–11.

Hall, J.G., 1997. Arthrogryposis multiplex congenita: etiology, genetics, classification, diagnostic approach, and general aspects. J. Pediatr. Orthop., B 6, 159–166.

Henry, E.W., Eicher, E.M., Sidman, R.L., 1991. The mouse mutation claw paw: forelimb deformity and delayed myelination throughout the peripheral nervous system. J. Heredity 82, 287–294.

Jacobson, L., Polizzi, A., Morriss-Kay, G., Vincent, A., 1999. Plasma from human mothers of fetuses with severe arthrogryposis multiplex congenita causes deformities in mice. J. Clin. Invest. 103, 1031–1038.

Jaegle, M., Mandemakers, W., Broos, L., Zwart, R., Karis, A., Visser, P., Grosveld, F., Meijer, D., 1996. The POU factor Oct-6 and Schwann cell differentiation. Science 273, 507–510.

Jaegle, M., Ghazvini, M., Mandemakers, W., Piirsoo, M., Driegen, S., Levavasseur, F., Raghoenath, S., Grosveld, F., Meijer, D., 2003. The POU proteins Brn-2 and Oct-6 share important functions in Schwann cell development. Genes Dev. 17, 1380–1391.

Jessen, K.R., Mirsky, R., 1991. Schwann cell precursors and their development. Glia 4, 185–194.

Jessen, K.R., Mirsky, R., 1999. Schwann cells and their precursors emerge as major regulators of nerve development. Trends Neurosci. 22, 402–410.

Jessen, K.R., Brennan, A., Morgan, L., Mirsky, R., Kent, A., Hashimoto, Y., Gavrilovic, J., 1994. The Schwann cell precursor and its fate: a study of cell death and differentiation during gliogenesis in rat embryonic nerves. Neuron 12, 509–527.

Koszowski, A.G., Owens, G.C., Levinson, S.R., 1998. The effect of the mouse mutation claw paw on myelination and nodal frequency in sciatic nerves. J. Neurosci. 18, 5859–5868.

Matthews, I., Sims, G., Ledwidge, S., Stott, D., Beeson, D., Willcox, N., Vincent, A., 2002. Antibodies to acetylcholine receptor in parous women with myasthenia: evidence for immunization by fetal antigen. Lab. Invest. 82, 1407–1417.

Moessinger, A.C., 1983. Fetal akinesia deformation sequence: an animal model. Pediatrics 72, 857–863.

Niemann, S., Sidman, R.L., Nave, K.A., 1998. Evidence against altered forms of MAG in the dysmyelinated mouse mutant claw paw. Mamm. Genome. 9, 903–904.

Parkinson, D.B., Dickinson, S., Bhaskaran, A., Kinsella, M.T., Brophy, P.J., Sherman, D.L., Sharghi-Namini, S., Duran Alonso, M.B., Mirsky, R., Jessen, K.R., 2003. Regulation of the myelin gene periaxin provides evidence for Krox-20-independent myelin-related signalling in Schwann cells. Mol. Cell. Neurosci. 23, 13–27.

Parmantier, E., Lynn, B., Lawson, D., Turmaine, M., Namini, S.S., Chakrabarti, L., McMahon, A.P., Jessen, K.R., Mirsky, R., 1999. Schwann cell-derived Desert hedgehog controls the development of peripheral nerve sheaths [see comments]. Neuron 23, 713–724.

Polizzi, A., Huson, S.M., Vincent, A., 2000. Teratogen update: maternal myasthenia gravis as a cause of congenital arthrogryposis. Teratology 62, 332–341.

Rushton, W.A., 1951. A theory of the effects of fibre size in medullated nerve. J. Physiol. 115, 101–122.

Saito, F., Moore, S.A., Barresi, R., Henry, M.D., Messing, A., Ross-Barta, S.E., Cohn, R.D., Williamson, R.A., Sluka, K.A., Sherman, D.L., Brophy, P.J., Schmelzer, J.D., Low, P.A., Wrabetz, L., Feltri, M.L., Campbell, K.P., 2003. Unique role of dystroglycan in peripheral nerve myelination, nodal structure, and sodium channel stabilization. Neuron 38, 747–758.

Scaravilli, F., Jacobs, J.M., 1981. Peripheral nerve grafts in hereditary leukodystrophic mutant mice (twitcher). Nature 290, 56–58.

Scherer, S.S., Salzer, J.L., 1996. Axon–Schwann cell interactions during peripheral nerve degeneration and regeneration. In: Jessen, K.R., Richardson, W.D. (Eds.), Glial Cell Development. Bios Scientific Publishers Ltd., Oxford, pp. 165–196.

Scherer, S.S., Xu, Y.T., Bannerman, P.G., Sherman, D.L., Brophy, P.J., 1995. Periaxin expression in myelinating Schwann cells: modulation by axon-glial interactions and polarized localization during development. Development 121, 4265–4273.

Seitz, R.J., Wechsler, W., Mosny, D.S., Lenard, H.G., 1986. Hypomyeli-

nation neuropathy in a female newborn presenting as arthrogryposis multiplex congenita. Neuropediatrics 17, 132–136.

Sherman, D.L., Brophy, P.J., 2000. A tripartite nuclear localization signal in the PDZ-domain protein L-periaxin. J. Biol. Chem. 275, 4537–4540.

Suter, U., Scherer, S.S., 2003. Disease mechanisms in inherited neuropathies. Nat. Rev., Neurosci. 4, 714–726.

Thomas, P.K., Berthold, C.-H., Ochoa, J., 1993. Microscopic anatomy of the peripheral nervous system. In: Dyck, P.J., Thomas, P.K. (Eds.), Peripher. Neuropathy, vol. 1. W.B. Saunders Company, Philadelphia, PA, pp. 28–73.

Topilko, P., Meijer, D., 2001. Transcription factors that control Schwann cell development and myelination. In: Jessen, K.R., Richardson, W.D. (Eds.), Glial Cell Development. Oxford Univ. Press, Oxford, pp. 223–244.

Webster, H.d., 1993. Development of peripheral nerve fibers. In: Dyck, P.J., Thomas, P.K., Griffin, J.W., Low, P.A., Poduslo, J.F. (Eds.), Peripheral Neuropathy. W.B. Saunders Company, Philadelphia, pp. 243–266.